Biosensors and Bioelectronics 141 (2019) 111405

Contents lists available at ScienceDirect

Biosensors and Bioelectronics

journal homepage: www.elsevier.com/locate/bios

A planar and uncharged copper(II)-picolinic acid chelate: Its intercalation to duplex DNA by experimental and theoretical studies and electrochemical sensing application

Juan Song[a], Jiancong Ni[a,b], Qinghua Wang[a], Huangcan Chen[c], Feng Gao[a,**], Zhenyu Lin[a,b], Qingxiang Wang[a,*]

[a] Department of Chemistry and Environment Science, Fujian Province University Key Laboratory of Analytical Science, Minnan Normal University, Zhangzhou, 363000, PR China

[b] Ministry of Education Key Laboratory of Analysis and Detection for Food Safety, Fujian Provincial Key Laboratory of Analysis and Detection for Food Safety, Fuzhou University, Fuzhou, 350116, China

[c] State Key Laboratory of Chemical Oncogenomics, Key Laboratory of Chemical Genomics, Peking University Shenzhen Graduate School, Shenzhen, 518055, China

ARTICLE INFO

Keywords:
Copper-picolinic acid
Hybridization indicator
Planar molecule
Molecular docking
Intercalation
Electrochemical DNA biosensor

ABSTRACT

Using an external redox-active molecule as a DNA hybridization indicator is still a popular strategy in electrochemical DNA biosensors because it is label-free and the multi-site binding can enhance the response signal. A planar and uncharged transition metal complex, $Cu(PA)_2$ (PA = picolinic acid) with excellent electrochemical activity has been synthesized and its interaction with double-stranded DNA (dsDNA) is studied by experimental electrochemical methods and theoretical molecular docking technology. The experimental results reveal that the copper complex interacts with dsDNA via specific intercalation, which is verified by the molecular docking result. The surface-based voltammetric analysis demonstrates that the planar $Cu(PA)_2$ can effectively accumulate within the electrode-confined hybridized duplex DNA rather than the single-stranded probe DNA. Based on this phenomenon, the $Cu(PA)_2$ is utilized as an electrochemical hybridization indicator for the detection of oligonucleotides. The sensing assays show that upon incubation in $Cu(PA)_2$ solution, the probe electrode does not display any Faraday signal, but the hybridized one has a pair of strong redox peaks corresponding to the electrochemistry of $Cu(PA)_2$, showing excellent hybridization indicating function of $Cu(PA)_2$ without background interference. The signal intensity of $Cu(PA)_2$ is dependent on the concentrations of the target oligonucleotide ranging from 1 fM to 100 nM with an experimental detection limit of 1.0 fM. Due to the specific intercalation of $Cu(PA)_2$ with dsDNA, the biosensor also exhibits good ability to recognize oligonucleotide with different base mismatching degree.

1. Introduction

The effective transformation of DNA hybridization event into a detectable electrochemical signal is a critical step in the construction of high-performance DNA biosensors (Li et al., 2018a,b; Zwang et al., 2018; Kumari et al., 2019). Typically, the analytical signals come from three types: signal tag labeled on probe strands (Hasegawa et al., 2017; Zhan et al., 2017), direct base oxidation/reduction (Maleh et al., 2015; Ahour et al., 2017), and external double-stranded and single-stranded DNA discriminator (namely hybridization indicator) (Ding et al., 2013; Balvedi et al., 2016). The biosensors with the signal tag labeled probe strands usually own excellent specificity, regenerability and stability, but the preparation of the probe strands are complicated. In addition, the signal molecule is tagged on the end of the probe strand by single-point conjunction, so the signal-output intensity, as well as sensitivity is limited. Another method to transfer the hybridization event is achieved by monitoring the electrochemistry variation of the internal purine bases, adenine or more often guanine upon hybridization reaction. Although the method is direct and facile, a high over-potential is required to achieve the electrochemical signals of these bases, which potentially causes the damage of the single-stranded probe DNA(ssDNA), and then decreases the regenerability of the biosensor. Alternatively, the biosensing strategy depending on the external indicator can be realized in an appropriate potential window by tuning the redox potential of the

* Corresponding author.
** Corresponding author.
E-mail address: axiang236@vip.163.com (Q. Wang).

https://doi.org/10.1016/j.bios.2019.111405
Received 4 May 2019; Received in revised form 30 May 2019; Accepted 1 June 2019
Available online 06 June 2019
0956-5663/

indicator. This detection process is label-free, which reduces the cost and saves the labor for the biosensor fabrication. What's more, the one-dimensional chain-like double-stranded DNA (dsDNA) has rich sites to accommodate numerous indicators, which is helpful for the sensor to gain high sensitivity. Therefore, using external hybridization indicators for DNA biosensing analysis is still a popular strategy in electrochemical DNA biosensor field.

Among the hybridization indicators, the metallo-intercalators (MIs) are one type of the most favorable ones due to their excellent redox reversibility, controllable geometrical configuration and high chemical stability. The MIs can bind with the DNA duplex rather than the unhybridized ssDNA through the specific intercalation mode. However, the currently developed MIs-based biosensors suffer from the following drawbacks: (1) To improve the specific intercalation of the MIs with dsDNA, the ligands with large aromatic ring like dipyrido[3,2-a:2′,3′-c] phenazine (dppz) (Maruyama et al., 2002; Li et al., 2015) are usually on demand. However, the complicated synthesis and low water solubility of these ligands block their practical application; (2) To enhance the signal intensity, some expensive and toxic redox-active metal ions like osmium(II) (Maruyama et al., 2002; Deféver et al., 2011) and ruthenium(II) (Dutse et al., 2012; Foo et al., 2017) have been used, which makes the biosensors not economic and environmental-friendly; (3) All above mentioned MIs are positively charged and can bind with the ssDNA through the non-specific electrostatic interaction, resulting in high background response for hybridization detection.

To address the above-mentioned problems, different strategies have been developed on the views of ligand screening, metal ions replacement and charge tuning. For example, Yang et al. (2015) replaced the intercalative ligand of DPPZ with commercial naphthalene diimide derivative and used the ferrocene as the redox-active moiety, which greatly simplifies the preparation process of the MIs. To reduce the preparing cost and the potential risk, many low-toxic and earth-abundant metal ions such copper(II) (Lin et al., 2011; Duprey et al., 2016), manganese(II) (Niu et al., 2009), and cobalt(II) (Wang et al., 2012a; Niu et al., 2013) have been utilized indicators preparation.

What's more, in order to avoid the non-specific electrostatic interaction between the positively charged MIs and negatively charged phosphates of DNA, Wong (Wong et al., 2003) has used a negatively charged 2,6-disulfonic acid anthraquinone (AQDS) as an indicator for DNA hybridization detection. The results show that the non-specific interaction of AQDS with ssDNA probe can be thoroughly eliminated due to their electrostatic repulsion. But it is unfortunate that, also because of the electrostatic repulsion, it will take ~12 h to finish the intercalative reaction of AQDS with hybridized DNA, which greatly hampers fast analysis of the biosensor. Also on the consideration of the nonspecific electrostatic interaction of MIs with DNA, our group has designed and synthesized a special MI for DNA analysis (Wang et al., 2013). The MI has two functional ligands, namely, glycollic acid (GA) and 1,10-phenathroline (phen): the planar aromatic ligand of phen is used for intercalation with dsDNA, and the GA is to compensate the positive charge of metal ions. The results show that, through the reasonable design of the charge-neutral MI, the background response during the hybridization detection can be effectively eliminated. However, the synthesis of the MI with mix-ligands is still complicated, and the steric hindrance of the charge-controlling ligand of GA weakens the interaction of the MI with dsDNA. Therefore, it is still a demand to design and synthesize simple and high-performance MI for electrochemical sensing analysis.

On this purpose, a copper(II) complex bearing two bidentate ligands of picolinic acid (PA) is synthesized through a simple one-step coordination reaction. As each ligand of PA has one negative charge, so the positive charges of center copper(II) ion can be totally compensated, and the complex is electroneutral. This can effectively prevent its non-specific electrostatic interaction with probe DNA. In addition, the geometric configuration of the complex consisting of tetra-coordinated Cu(II) and two PA ligands presents the well-defined planar structure, making the complex intercalating into DNA duplex as a whole without any steric hindrance. On the basis of this, the MI was utilized as an electrochemical indicator to monitor the hybridization of DNA. The target DNA can be detected in a wide range from 1 fM to 100 nM with the experimental detection limit of 1.0 fM. Due to the specific intercalation of $Cu(PA)_2$ with dsDNA and absence of background response, the biosensor also exhibits good ability to recognize oligonucleotides with different base mismatching degree, showing the promising practical application of the developed biosensor.

2. Experimental

2.1. Reagents and apparatus

Native fish-sperm DNA (fsDNA) was purchased from Beijing Baitai Biochemistry Technology Company (China) and used as received. The concentration of the DNA in the nucleotide phosphate (NP) was determined spectrophotometrically at 260 nm using the known molar extinction coefficient of 6600 M^{-1} cm^{-1} (Reichman et al., 1954). The 18-base synthetic oligonucleotides were purchased from Shanghai Sangon Bioengineering Co., Ltd. (China). The $Cu(PA)_2$ was synthesized through a homogeneous reaction under ambient temperature as we reported in previous work (Wang et al., 2012b). The detailed synthesis procedure of $Cu(PA)_2$ and the other material information are given in Supplementary Materials.

Electrochemical experiments were carried out on a CHI 650C electrochemical workstation (China) consisting of traditional three-electrode system: bare or DNA-modified glassy carbon electrode (GCE, Φ = 3 mm) as a working electrode, a Ag/AgCl as the reference electrode and a Pt wire as the counter electrode.

2.2. Experimental studies on the interaction of $Cu(PA)_2$ with native dsDNA

The interaction mechanism including binding mode, binding site and binding constant of the synthesized $Cu(PA)_2$ with dsDNA was experimentally studied by different electrochemical technologies like cyclic voltammetry (CV), normal pulse voltammetry (NPV), chronocoulometric (CC) and differential pulse voltammetry (DPV) measurements. In detail, to an aqueous solution of $Cu(PA)_2$ containing 20 mM BR buffer (pH 7.0), an appropriate amount of dsDNA was added and then reacted for 10 min under ambient condition. Then the solution was electrochemically scanned by above-mentioned methods.

2.3. Molecular docking of $Cu(PA)_2$ with dsDNA

The molecular docking experiments of $Cu(PA)_2$ to dsDNA were performed with Auto Dock vina software. The best DNA-$Cu(PA)_2$ configurations was achieved by comparing several scoring criteria such as affinity, binding site and binding orientation. Two DNA sequences, d(CGCGAATTCGCG)$_2$ (PDB ID: 1BNA) and d(CGATCG)$_2$ (PDB ID: 1Z3F) selected from the Protein Data Bank (PDB) (RCSB) were used as models for groove binding and intercalation docking, respectively. With the aid of Auto Dock tools, all hydrogen atoms and Gasteiger charges were added. This structure was further modified for docking calculations through Auto Dock vina. All of the water molecules were removed, whereas the Gasteiger charges and essential hydrogen atoms were added. A total of 20 models were accomplished, and the best structure with the lowest binding free energy was used. The crystal structure of $Cu(PA)_2$ (CCDC: 838907) was taken from its X-ray diffraction data (Wang et al., 2012b), and the PDB format of the complex was obtained by converting the complex's CIF file using Mercury software.

2.4. Fabrication of the biosensor and the hybridization reaction

The biosensor was fabricated by covalent immobilization of amino-modified oligonucleotide probe (pDNA) on the carboxylated GCE. First,

the GCE was cleaned through routine physical polishing and ultrasonication washing. Then, the cleaned GCE was polarized at +1.5 V for 15 s in a strong acid mixture containing 2.5% $K_2Cr_2O_7$ and 10% HNO_3 to produce the functional carboxyl groups (-COOH) at the electrode surface (Gao et al., 2013). Thereafter, 20 μL PBS containing 5 mM NHS and 8 mM EDC was dropped on the electrode surface and dried at room temperature to activate the functional oxygen-containing groups. After that, 10 μL of 10 μM pDNA solution was cast onto the electrode surface and the top of the electrode was coved with an Eppendorf tube. After reaction for 3 h, the electrode was rinsed with PBS to eliminate the nonspecifically adsorbed DNA. The obtained modified electrode was denoted as pDNA/GCE.

The hybridization reaction was performed by immersing pDNA/GCE into 20 mM TE buffer containing different sequences for 1 h at 42 °C with gentle shaking. Then the hybridized electrodes were washed with PBS to remove the unhybridized DNA.

2.5. Indicator binding and hybridization measurements

The indicator binding was carried out by immersing the hybridized and unhybridized DNA-modified electrode into a pH 7.0 BR buffer containing 1.5 mM $Cu(PA)_2$ for 10 min for binding equilibrium, and then the electrodes were transferred into 20 mM pH 7.0 BR buffer free of the copper complex for CV and DPV measurements. The potential of CV range from −0.2 V to +0.6 V with the scan rate of 100 mV s^{-1}. The DPV was recorded within the potential range from +0.1 V to +0.5 V.

3. Results and discussion

3.1. Synthesis, structure of $Cu(PA)_2$ and working principle of the biosensor

The copper(II) complex, as a class of common transition metal compounds, receives considerable interest in bioinorganic chemistry and analytical chemistry due to their bioactivity, and excellent spectroscopic and electrochemical properties. The PA-based copper(II) complexes have been widely studied as the DNA-targeted molecules (Pulimamidi et al., 2014; Parveen et. al. 2014). In this work, the simple binary copper(II) complex, $Cu(PA)_2$ is synthesized and utilized as the electrochemical probe. Fig. 1A shows the synthesis route of the copper complex. It is obtained through a simple chelating reaction of bidentate ligand of PA with the center ion of Cu^{2+}. Through the stoichiometric ratio of 1:2 (Cu^{2+}:PA), the planar complex of $Cu(PA)_2$ is achieved. In addition, since two negatively charged PA ligands balance the positive charges of Cu^{2+}, the complex of $Cu(PA)_2$ presents electroneutrality as a whole. Fig. 1B shows the ORTEP view of $Cu(PA)_2$ with 30% thermal ellipsoid probability. It is observed that the copper(II) complex consists of two deprotonated bidentate PA ligands and one uncoordinated water molecule occupying lattice sites. The Cu atom lies in the center of a distorted N_2O_2 square formed by two N atoms and two O atoms from two PA ligands. The bond angles of O3–Cu1–O3a and N1–Cu1–N1a are resolved to be 180°, confirming that the $Cu(PA)_2$ presents a planar structure. More information concerning the crystal structure of the complex can be obtained from our previously reported work (Wang et al., 2012b).

Based on the above structure characteristic of $Cu(PA)_2$, an electrochemical biosensor using $Cu(PA)_2$ as a hybridization indicator is designed. Fig. 1C shows the construction and its working principle for the detection of target DNA (tDNA). First, the pDNAs were immobilized onto the surface of GCE by the condensation reaction between –COOH and amino (-NH_2) under the assistance of EDC/NHS. Then the tDNA was hybridized to form duplex structure. When the hybridized electrode was incubated in $Cu(PA)_2$ solution, the planar $Cu(PA)_2$ specifically bind with dsDNA, and an electrochemical response corresponding to the intercalated $Cu(PA)_2$ is monitored. Since the single-stranded probe DNA has no binding site for $Cu(PA)_2$, the obtained signal on the electrode surface can be directly applied as an indicating signal for hybridization. Based on this principle, a simple, sensitive, easy-operation and cost-effective biosensor can be developed.

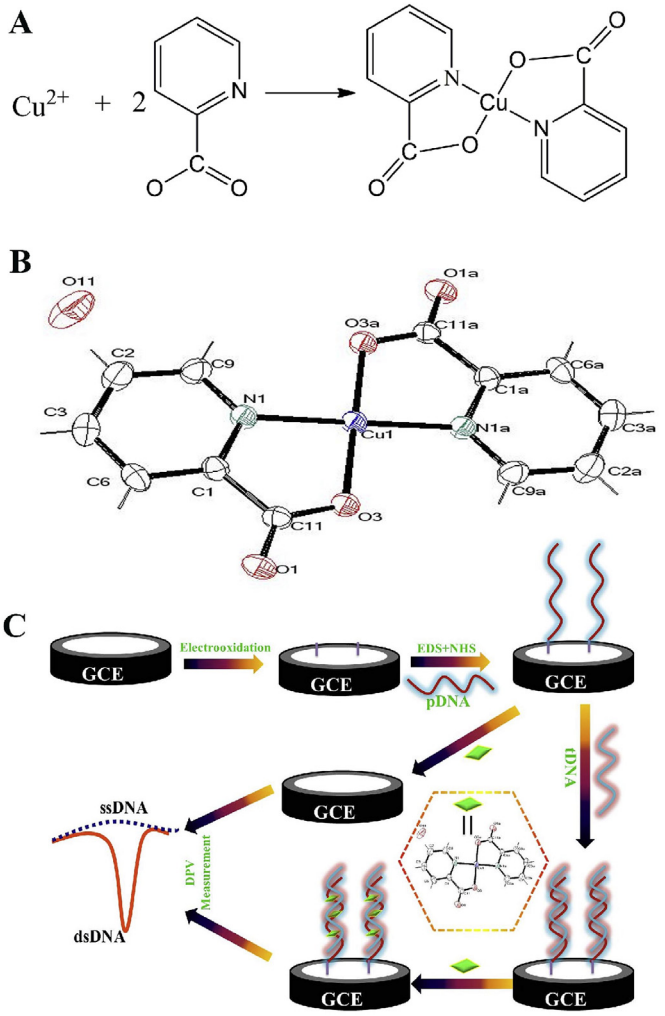

Fig. 1. (A) Synthesis route of the copper complex, $Cu(PA)_2$. (B) ORTEP view of $Cu(PA)_2{\cdot}H_2O$ with 30% thermal ellipsoid probability. (C) Fabrication and working principle of the DNA biosensor using $Cu(PA)_2$ as the hybridization indicator.

3.2. Binding mechanism of $Cu(PA)_2$ with fsDNA in solution by electrochemistry

Different electrochemical methods were applied to investigate the interaction mode of the $Cu(PA)_2$ with DNA duplex in solution using native fish-sperm DNA (fsDNA) as model. Fig. 2A shows the typical CVs of 200 μM $Cu(PA)_2$ before (a), and after interaction with 80 μM (b) and 150 μM (c) fsDNA in 20 mM BR buffer (pH 7.0). It is found that $Cu(PA)_2$ has a pair of well-defined redox peaks at +0.318 V and +0.138 V. respectively (curve a), which is assigned to the electron transfer couple of Cu(II)/Cu(I) (Zhan et al., 2017; Song et al., 2018). The potential difference of the two peaks is 180 mV, and the peak current ratio ($|I_{pa}/I_{pc}|$) is close to 1, suggesting that the electrochemical behavior of the $Cu(PA)_2$ is a quasi-reversible process. When 80 μM fsDNA is injected, the redox peaks of $Cu(PA)_2$ decrease remarkably, suggesting $Cu(PA)_2$ has reacted with fsDNA, which is confirmed by the further decrease of the redox signal by adding 150 μM fsDNA. According to equations (1), the formal potentials of $Cu(PA)_2$ before and after binding with 150 μM fsDNA are calculated to be +90 mV and +104 mV, respectively. The positive shift of the formal potential suggests the possible intercalative interaction between $Cu(PA)_2$ and fsDNA (Carter et al., 1989), and this

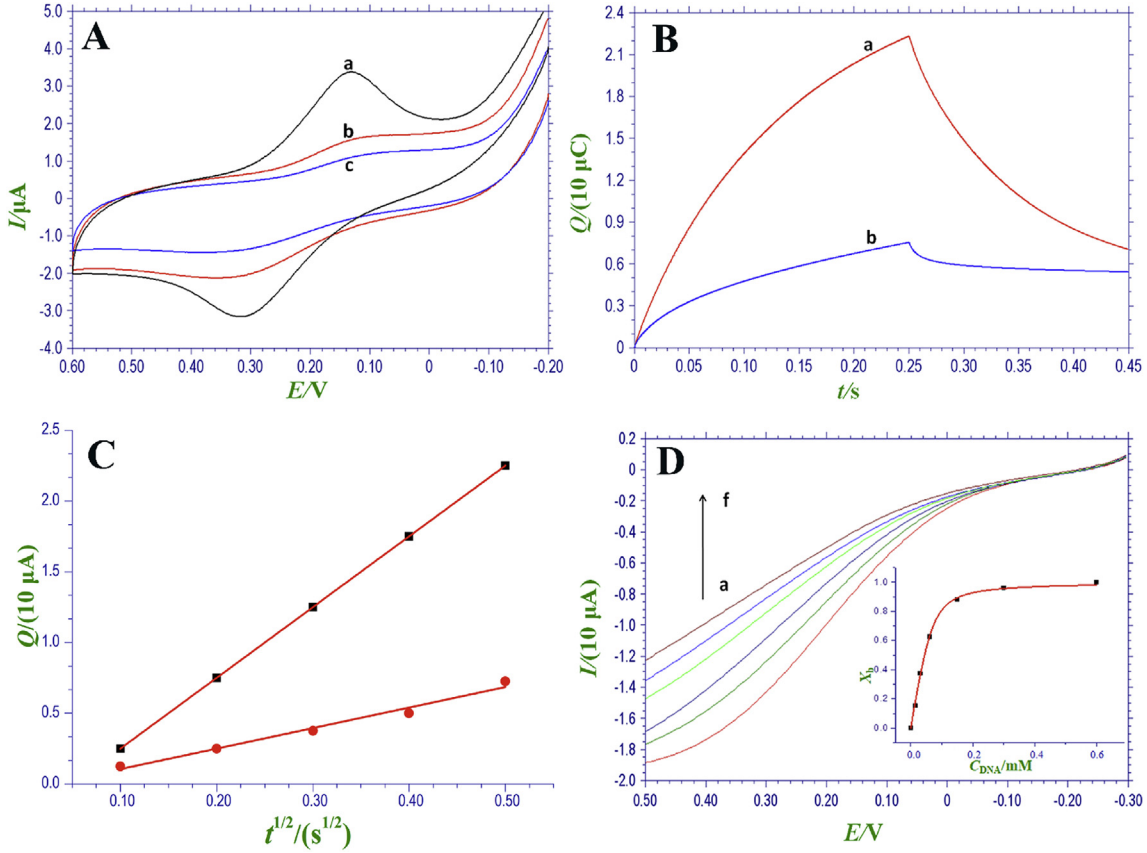

Fig. 2. (A) CVs of 8 mL 20 mM BR buffer (pH 7.0) containing 200 μM $Cu(PA)_2$ without (a), and with 80 μM (b) and 150 μM (c) DNA. (B) CCs of 200 μM $Cu(PA)_2$ before (a) and after (b) reacted with 800 μM DNA. (C) The plots of Q versus $t^{1/2}$. (D) NPVs of 20 μM $Cu(PA)_2$ upon titration with 0 (a), 3.30 μM (b), 13.4 μM (c), 26.7 μM (d), 40.1 μM (e), 60.1 μM (f), and 100 μM (g) DNA. Inset: The plot of X_b versus DNA concentration ([DNA]).

conclusion is also consistent with the result judged from the binding constant ratio (K_{Red}/K_{Ox}) of the reduction state of $Cu(PA)_2$ with fsDNA to that of the oxidation state (see the detail discussion in Supplementary Material)

$$E^{\theta'} = \left(\frac{E_{pa} + E_{pc}}{2}\right) \quad (1)$$

Chronocoulometry was carried out to calculate the diffusion coefficients (D) of $Cu(PA)_2$ and $Cu(PA)_2$-dsDNA. Fig. 2B shows the typical CC curves of 200 μM $Cu(PA)_2$ before (a) and after (b) reaction with excess (800 μM) fsDNA. The plots of total charge (Q) versus the square root of the potential pulse width ($t^{1/2}$) for $Cu(PA)_2$ and $Cu(PA)_2$-fsDNA are depicted in Fig. 2C. From the slopes of the two plots, the D values of the two systems are calculated to be $8.75 \times 10^{-5}\,cm^2\,s^{-1}$ and $2.40 \times 10^{-5}\,cm^2\,s^{-1}$, respectively, suggesting that the diffusion kinetics of $Cu(PA)_2$ is decreased by 72.6% after formation complex with fsDNA. This result confirms the interaction of $Cu(PA)_2$ and fsDNA, and the formation of the adduct decreases the diffusion kinetics of $Cu(PA)_2$.

Furthermore, the binding parameters of $Cu(PA)_2$ to fsDNA are investigated through an NPV titration method. Fig. 2D shows the NPVs of the $Cu(PA)_2$ upon interaction with increasing concentrations of fsDNA. Obviously, the limiting diffusion currents decrease gradually with the increase of fsDNA concentration and finally reach to the steady-state minimum values. The binding parameters such as binding constant (K) and binding site size (s) are then calculated through the NPV data and corresponding equations (3–5) (Johnston et al., 1996):

$$X_b = \{b - (b^2 - 2K^2 - C_{Cu}[NP])/s^{1/2}\}/2KC_{Cu} \quad (2)$$

$$X_b = (I^2 - I_{int}^2)/(I_{sat}^2 - I_{int}^2) \quad (3)$$

$$b = 1 + KC_{Cu} + K[NP]/2s \quad (4)$$

where X_b is the molar binding fraction, I the limiting current upon interaction with fsDNA, I_{int} the initial current without the addition of fsDNA, I_{sat} the current upon binding saturation with DNA. C_{Cu} is the total concentration of $Cu(PA)_2$, and [NP] is the concentration of the added fsDNA. From the NPV results, the relationship of X_b versus [NP] is plotted as inset of Fig. 2D. Then the value of K is estimated to be 3.1 ($\pm$ 0.9) $\times 10^5\,M^{-1}$ through nonlinear fitting analysis of equations (2)–(4). This result qualitatively suggests that the copper complex bound to fsDNA with a strong strength, which is in agreement with the affinity of other intercalators (Phadte et al., 2019; Yaghobi et al., 2019). Additionally, the value of s is obtained to be 1.7 ($\pm$ 0.1), which indicates that two adjacent base pairs accommodate one $Cu(PA)_2$ molecule. This result also demonstrates that when the $Cu(PA)_2$ is utilized as a hybridization indicator, the multiple site binding mode, in comparison with the single-point labeled molecular beacon probe, can increase loading amount of signal molecules and improve the electrochemical output response in hybridization analysis. In addition, since the $Cu(PA)_2$ is a planar molecule as a whole, its binding site size (s = 1.7) is smaller than those of the other indicators such as $Co(phen)_3^{3+}$ (s = 6) (Millan et al., 1993), bisnaphthyl imide tetracationic diviologen compound (s = 6.1) (Hvastkovs et al., 2007) and bi-acetylferrocene ethylenediamine complex (s = 4.2) (Ding et al., 2013), suggesting that the DNA duplex with the same length can accommodate much more $Cu(PA)_2$ to produce stronger electrochemical response as well as higher analytical sensitivity in sensing analysis.

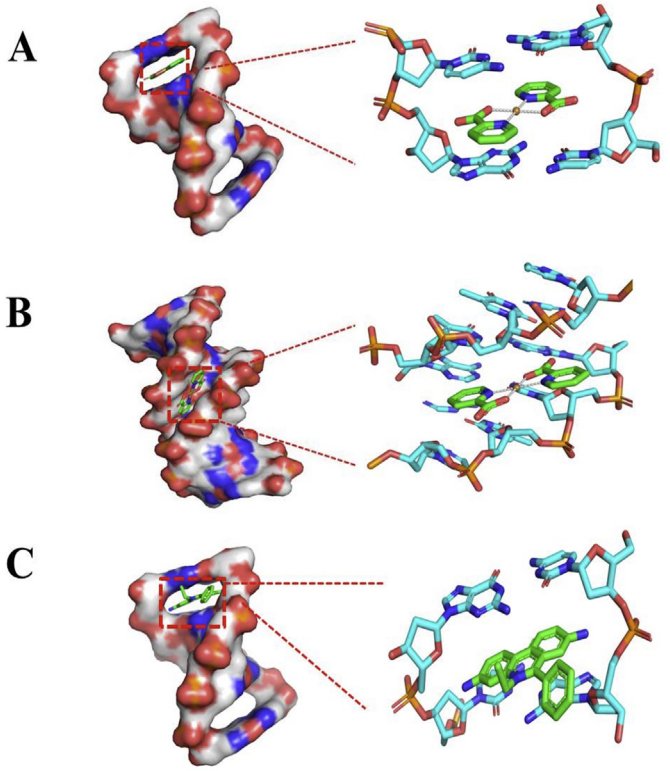

Fig. 3. The docked pose of $Cu(PA)_2$ complexes bound to the minor groove (A) and intercalation (B) mode with DNA. And docked pose of a classic intercalator of EtBr (C).

3.3. Molecular docking calculation on the binding of $Cu(PA)_2$ with duplex DNA

To verify the conclusion of intercalative binding of $Cu(PA)_2$ with duplex DNA from electrochemical experiments, the molecular docking studies were performed. The preferred binding site and best orientation of the molecules on the DNA structure are determined by the minimum energy of $Cu(PA)_2$-dsDNA complex. By the Auto Dock Vina software, the docking result of $Cu(PA)_2$ with dsDNA at two possible binding modes (groove binding and intercalation) are illustrated in Fig. 3A and Fig. 3B, respectively. As a control, the docking of a classic intercalator, ethidium bromide (EtBr) with dsDNA was also performed, and the result is displayed in Fig. 3C. Then from the docking results, the binding scores of $Cu(PA)_2$ and EtBr with dsDNA at different sites were calculated, and the results are given as Table S1 in Supplementary Material. As seen, the $Cu(PA)_2$ presents a binding score of $-7.7\ kcal\ mol^{-1}$ at intercalation mode, which is obviously smaller than that of the groove binding mode ($-7.0\ kcal\ mol^{-1}$), confirming that the planar $Cu(PA)_2$ is preferred to bind with dsDNA via the intercalation (Li et al., 2018a,b). And even, the binding score of $Cu(PA)_2$ in lower than that of EtBr ($-7.3\ kcal\ mol^{-1}$), suggesting that the $Cu(PA)_2$ has a stronger affinity with dsDNA than the classic intercalator of EtBr. Such strong intercalation is expected to improve the stability of the biosensor when $Cu(PA)_2$ is applied as an indicator for hybridization detection as the bound $Cu(PA)_2$ is not easy to dissociate from the electrode surface during rinsing and test process.

3.4. Electrochemical recognition of $Cu(PA)_2$ toward dsDNA and ssDNA

Above homogeneous solution studies and molecule docking analysis have shown that the copper complex interacts with dsDNA through the intercalative mode. The intercalation is a specific mode that only happens with dsDNA rather than ssDNA because the intercalation site

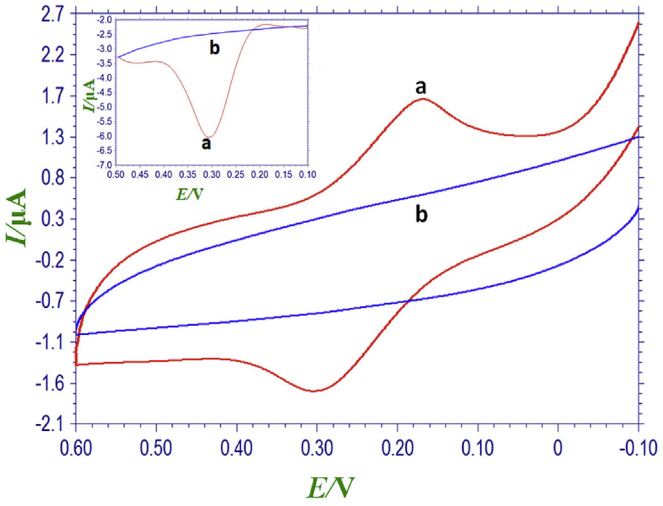

Fig. 4. CVs (main panel) and DPVs (inset) of pDNA/GCE (a) and tDNA-pDNA/GCE (b) with pre-accumulated $Cu(PA)_2$ in 20 mM pH 7.0 BR buffer.

(*i.e.*, the base pairs) is only present in dsDNA. So it is speculated that the copper complex can be used as an electrochemical probe for structure recognition of dsDNA and ssDNA. In order to further testify this speculation, the interaction of $Cu(PA)_2$ with dsDNA and ssDNA was investigated on the electrode surface. Fig. S1 shows the multi-sweep CVs of pDNA/GCE (A) and tDNA-pDNA/GCE (B) in 200 μM $Cu(PA)_2$. It is observed that on pDNA/GCE, a couple of obscure redox peak appears and the redox signals are hardly changed with increase of scan cycles. In contrast, when tDNA-pDNA/GCE was tested in the same conditions, the redox peaks of $Cu(PA)_2$ enhance gradually with increase of the scan cycles. This difference demonstrates that increasing amounts of Cu $(PA)_2$ molecules are accumulated on the dsDNA modified electrode rather than ssDNA electrode with increase of the accumulation time.

The electrochemistry of pDNA/GCE and tDNA-pDNA/GCE with fully absorbed $Cu(PA)_2$ was also investigated in a blank BR buffer, which can eliminate the signal interference from the direct diffusion of $Cu(PA)_2$ from the bulk solution to the electrode surface. The CVs (main panel) and DPVs (inset) results are displayed in Fig. 4. As depicted, there is not any evident Faraday's peak at the pDNA/GCE (curve a), showing there is not $Cu(PA)_2$ adsorbed on pDNA/GCE. However, a pair of strong redox peak in CV and well-defined oxidation peak in DPV is present on tDNA-pDNA hybridized electrode (curve b). These results indicate that no background interference is produced for the biosensor when the planar and uncharged $Cu(PA)_2$ was utilized as hybridization indicator. This is obviously superior to the other biosensors using positively-charged molecules as the indicators (Niu et al., 2013; Duprey et al., 2016; Nagy et al., 2018). It is also noticeable that the absolute binding of $Cu(PA)_2$ on hybridized electrode can be finished in 10 min (Fig. S2 in Supplementary Material), which is extremely shorter than the negatively charged indicator like AQDS (~12 h) (Wong et al., 2003), and even some positively charged indicators like $[Co(phen)_2(Cl)(H_2O)]^+$ (20 min) (Niu et al., 2013), bisnaphthyl imide tetracationic diviologen compound (30 min) (Hvastkovs et al., 2007), and $[Cu(bpy)(MBZ)_2(H_2O)]$ (20 min) (Wang et al., 2011). This can be explained by the electroneutral and planar characteristic of $Cu(PA)_2$ as a whole, which bypass the electrostatic repulsion of negatively charged indicators and the steric hindrance effect of the mix-liganded indicators.

3.5. Analytical performance

Under the optimal concentration (1.5 mM) of $Cu(PA)_2$ (Fig. S3 in Supplementary Material), the analytical performance of the biosensor for target DNA is investigated. Fig. 5A shows the anodic DPVs of Cu $(PA)_2$ on the biosensor upon hybridization with various concentrations

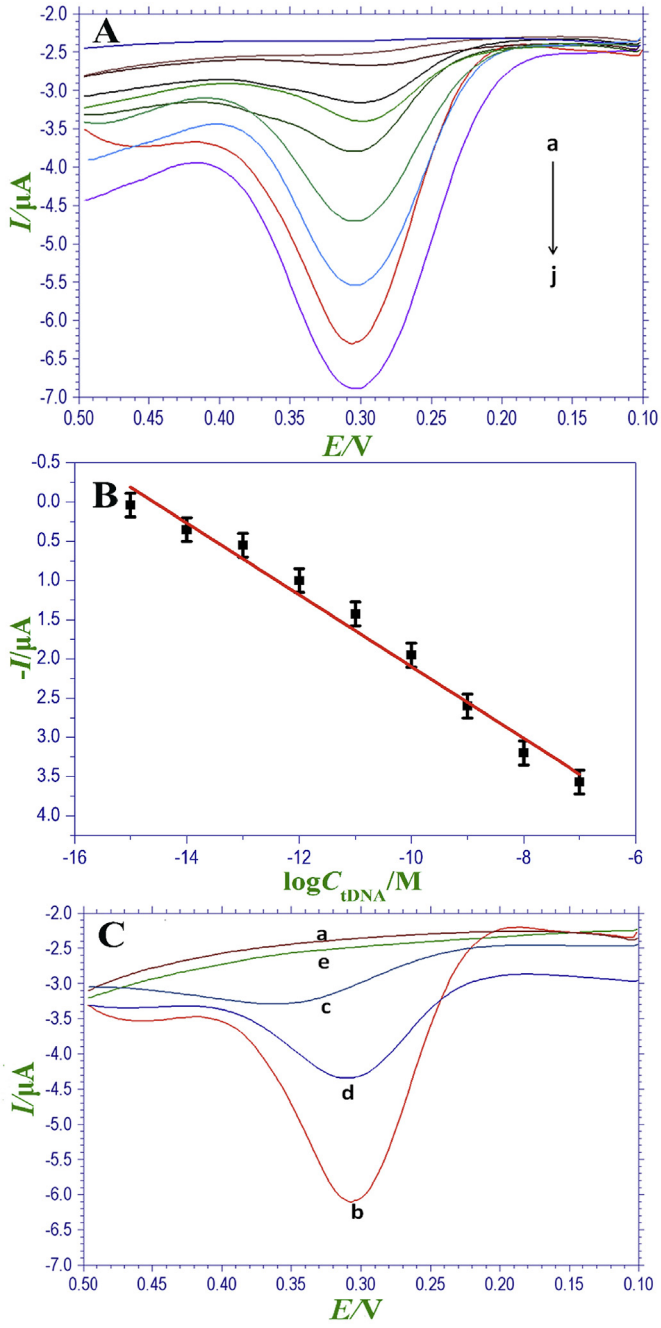

Fig. 5. (A) DPVs of 1.5 mM $Cu(PA)_2$ accumulated on pDNA/GCE upon hybridization with 0 (a), 1 fM (b), 10 fM (c), 0.1 pM (d), 1.0 pM (e), 10 pM (f), 0.1 nM (g), 1.0 nM (h), 10.0 nM (i), 100 nM (j) tDNA. (B) Linear relationship of the oxidation peak currents ($-I_p$) versus the logarithm value of tDNA (log C_{tDNA}). (C) DPVs $Cu(PA)_2$ recorded on pDNA/GCE before (a) and after hybridization with 10 nM tDNA (b), 0.1 μM omDNA (d), 0.1 μM tmDNA (c) and 0.1 μM nDNA (e).

of tDNA. It is found that on the probe electrode, not any Faraday's signal is observed, suggesting that the probe electrode totally has not adsorption on $Cu(PA)_2$. Then the oxidation peak arouses from the Cu $(PA)_2$ couple increases gradually when the biosensor hybridizes with increasing concentration of the tDNA. This suggests that the electrochemical signals achieved on the biosensor are strictly dependent on the hybridization reaction of the biosensor with target DNA. In addition, the peak currents (I_p) and the logarithm of tDNA concentrations (logC_{tDNA}) is in a good linear relationship in the range from 1.0 fM to 100 nM (Fig. 5B) with a regression equation of $I_{pa}/(\mu A)$ = -0.46log (C_{tDNA}/M)-6.71, R = 0.9895. The theoretic limit of detection (LOD) is estimated to be 100 aM based on the rule of three times standard deviation of background signals. However, when this value was put into the linear regression equation, an unreasonable result, *i.e.* a positive value of peak current (+0.65 μA) is obtained. Actually, the value for the oxidation peak should be a negative value in this work. The reason might be that the peak current value for the concentration of 1.0 fM tDNA is very close to zero. So, the extremely low experimental concentration of 1.0 fM that can be truly detected was adopted as the LOD of the biosensor (Wan et al., 2015; Rizwan et al., 2018), we adopted the lowest experimental value (1.0 fM) as the LOD. Table S2 in Supplementary Material shows the comparison of the analytical performance of DNA biosensors using different hybridization indicators. Clearly, the biosensor developed in this work presents the widest linear range and the lowest detection limit, which is likely attributed to the excellent electroactivity of $Cu(PA)_2$ molecule, its specific intercalation with hybridized DNA, and absence of background response on probe electrode.

In addition, from the previous experiment and theoretic calculation, it is known that $Cu(PA)_2$ binds with dsDNA via intercalation into the adjacent base pairs. Thus it is expected that in this work, for the DNA fragments with the same base length, the more intact hybridized strands, the more intercalative sites there are to accommodate the Cu $(PA)_2$, and then the larger electrochemical signal will be produced. Based on this feature, the monitoring ability of the biosensor using Cu $(PA)_2$ as the hybridization indicator to base mutation is investigated. When the target DNA fragments with different base-mismatching degrees are utilized as models, the analytical results are displayed in Fig. 5C. As we can see, when the non-complementary DNA is hybridized with probe DNA on the biosensor, no oxidation peak appears (curve e), as the same response on pDNA/GCE (curve a), which indicates that the hybridization reaction does not happen between pDNA and the non-complementary DNA. In addition, it is worth noting that even if the non-complementary DNA has non-specific adsorption on the sensor surface, it will also not produce any Faraday's response from $Cu(PA)_2$, as no intercalative site is formed at this case. However, when pDNA/GCE was hybridized with the perfectly complementary sequence of tDNA, the electrochemical response of the complex enhances greatly (curve b), terrifying that the $Cu(PA)_2$ has been well captured by the hybridized duplex DNA. Alternatively, when the electrode was hybridized with one-base mismatching sequences of omDNA (curve d), the detected signal is significantly decreased compared with tDNA-pDNA/GCE, owing to the formation of the imperfect double helix structure which reduces the binding sites for $Cu(PA)_2$. When the electrode was hybridized with a three-base mismatching sequence of tmDNA (curve c), the response is further decreased. These results indicate that the biosensor is capable of recognizing target DNA with different mutation degree. Unfortunately, as the signal of the developed biosensor is based on the intercalated $Cu(PA)_2$ on hybridized DNA duplex, it is still hard to get the information concerning the detailed mutation site and the number of the base by the present method.

4. Conclusions

In this work, a copper complex, $Cu(PA)_2$ with the characteristic of electron-neutrality, perfect planarity and excellent redox response has been utilized as a hybridization indicator in DNA detection. Molecule docking study shows that the planar $Cu(PA)_2$ preferably interacts with dsDNA via the intercalation rather than groove binding, and even the affinity is larger than the classic intercalator of EtBr. The surface-based electrochemical studies further demonstrate that the complex can well discriminate dsDNA from ssDNA. In DNA hybridization detection, when the $Cu(PA)_2$ is utilized as the hybridization indicator, a faster binding process in comparison with traditional negative and mix-liganded intercalators, since its electroneutral feature and better planarity as a whole. In addition, because the intercalation of $Cu(PA)_2$ into dsDNA is strictly depended on the formation of the duplex structure of DNA, so

not any background signal is observed on probe electrode, and an ultralow detection limit (1 fM) is achieved. These advatanges make the Cu $(PA)_2$-based biosensor promising for practical application in early screening, diagnosis, and prognosis of gene patients, and the its applicability in the real samples such as serum, urine or other biological extracation solutions will be our future research.

5. Declaration of interests

The authors declare that they have no known competing financial interests or personal relationships that could have appeared to influence the work reported in this paper.

CRediT authorship contribution statement

Juan Song: Methodology, Writing - original draft. **Jiancong Ni:** Data curation. **Qinghua Wang:** Formal analysis. **Huangcan Chen:**Software. **Feng Gao:** Writing - review editing, Supervision. **Zhenyu Lin:** Writing - review editing. **Qingxiang Wang:** Conceptualization, Writing - review editing, Supervision.

Acknowledgments

We gratefully acknowledge financial support from the National Natural Science Foundation of China (21802064, 21775026, 21275127) and Natural Science Foundation of Fujian Province, China (2018J01435).

Appendix A. Supplementary data

Supplementary data to this article can be found online at https://doi.org/10.1016/j.bios.2019.111405.

References

Ahour, F., Shamsi, A., 2017. Anal. Biochem. 532, 64–71.
Balvedi, R.P.A., Caetano, L.P., Madurro, J.M., Madurro, A.G.B., 2016. Biosens. Bioelectron. 85, 226–231.
Carter, M.T., Rodriguez, M., Bard, A.J., 1989. J. Am. Chem. Soc. 111, 8901–8911.
Deféver, T., Druet, M., Evrard, D., Marchal, D., Limoges, B., 2011. Anal. Chem. 83, 1815–1821.
Ding, Y.T., Wang, Q.X., Gao, F., Gao, F., 2013. Electrochim. Acta 106, 35–42.
Duprey, J.L.H.A., Carr－Smith, J., Horswell, S.L., Kowalski, J., Tucker, J.H.R., 2016. J. Am. Chem. Soc. 138, 746–749.
Dutse, S.W., Yusof, N.A., Ahmad, H., Hussein, M.Z., Zaina, Z., 2012. Int. J. Electrochem. Sci. 7, 8105–8115.
Foo, K.L., Kashif, M., Tan, S.J., Hashim, U., 2017. Microsyst. Technol. 23, 1237–1245.
Gao, F., Cai, X.L., Wang, X., Gao, C., Liu, S.L., Gao, F., Wang, Q.X., 2013. Sensor. Actuator. B Chem. 186, 380–387.
Hasegawa, Y., Takada, T., Nakamura, M., Yamana, K., Bioorg, 2017. Med. Chem. Lett. 27, 3555–3557.
Hvastkovs, E.G., Buttry, D.A., 2007. Anal. Chem. 79, 6922–6926.
Johnston, D.H., Thorp, H.H., 1996. J. Phys. Chem. 100, 13837–13843.
Kumari, P., Adeloju, S.B., 2019. Talanta 194, 127–133.
Li, C.X., Wang, H.Y., Shen, J., Tang, B., 2015. Anal. Chem. 87, 4283–4291.
Li, X., Chen, B., Lan, L., Wang, R., Luo, D., Liu, L., Cheng, L., 2018a. Chin. Chem. Lett. 29, 1637–1640.
Li, Y.R., Chang, Y.Y., Yuan, R., Chai, Y.Q., 2018b. ACS Appl. Mater. Interfaces 10, 25213–25218.
Lin, L.Q., Kang, J., Weng, S.H., Chen, J.H., Liu, A.L., Lin, X.H., Chen, Y.Z., 2011. Sensor. Actuator. B Chem. 155, 1–7.
Maleh, H.K., Javazmi, F.T., Atar, N., Yola, M.L., Gupta, V.K., Ensafi, A.A., 2015. Ind. Eng. Chem. Res. 54, 3634–3639.
Maruyama, K., Mishima, Y., Minagawa, K., Motonaka, J., 2002. Anal. Chem. 74, 3698–3703.
Millan, K.M., Mikkelsen, S.R., 1993. Anal. Chem. 65, 2317–2323.
Nagy, L.K., Sørensen, K.D., Ferapontov, E.E., 2018. Biosens. Bioelectron. 117, 444–449.
Niu, S.Y., Zhao, M., Ren, R., Zhang, S.S., 2009. J. Inorg. Biochem. 103, 43–49.
Niu, S.Y., Sun, J., Nan, C.C., Lin, J.H., 2013. Sensor. Actuator. B Chem. 176, 58–63.
Parveen, S., Arjmand, F., Ahmad, I., 2014. J. Photochem. Photobiol., B 130, 170–178.
Phadte, A.A., Banerjee, S., Mate, N.A., Banerjee, A., 2019. Biochem. Biophys. Rep. 18, 100629.
Pulimamidi, R.R., Nomula, R., Pallepogu, R., Shaik, H., 2014. Eur. J. Med. Chem. 79, 117–127.
Reichman, M.E., Rice, S.A., Thomas, C.A., Doty, P., 1954. J. Am. Chem. Soc. 76, 3047–3053.
Rizwan, M., Elma, S., Lim, S.A., Ahmed, M.U., 2018. Biosens. Bioelectron. 107, 211–217.
Song, Y.H., Xu, M.L., Gong, C.C., Shen, Y., Wang, L.Y., Xie, Y., Wang, L., 2018. Sensor. Actuator. B Chem. 257, 792–799.
Wan, Y., Wang, P.J., Su, Y., Wang, L.H., Pan, D., Aldalbahi, A., Yang, S.L., Zuo, X.L., 2015. ACS Appl. Mater. Interfaces 7, 25618–25623.
Wang, Q.X., Shi, J.L., Ni, J.C., Gao, F., Gao, F., Weng, W., Jiao, K., 2011. Electrochim. Acta 56, 3829–3834.
Wang, Q.X., Gao, F., Gao, F., Li, S.X., Weng, W., Liu, F.Q., Jiao, K., 2012a. Biosens. Bioelectron. 32, 50–55.
Wang, Q.X., Yu, Z.L., Wang, Q.H., Li, W.Q., Gao, F., Li, S.X., 2012b. Inorg. Chim. Acta 383, 230–234.
Wang, Q.X., Ding, Y.T., Wang, L.H., Ni, J.C., Yu, Z.L., Lin, H.B., Gao, F., 2013. Chem.－Asian J. 8, 1455–1462.
Wong, E.L.S., Gooding, J.J., 2003. Anal. Chem. 75, 3845–3852.
Yaghobi, Z., Ranjbar, Z.R., Gharbi, S., 2019. Polyhedron 164, 176–184.
Yang, Z.G., Auriac, M.A., Goggins, S., Hordern, B.K., Thomas, K.V., Frost, C.G., Estrela, P., 2015. Environ. Sci. Technol. 49, 5609–5617.
Zhan, F.P., Liao, X.L., Gao, F., Qiu, W.W., Wang, Q.X., 2017. Biosens. Bioelectron. 92, 589–595.
Zwang, T.J., Tse, E.C.M., Barton, J.K., 2018. ACS Chem. Biol. 13, 1799－1809.